摩耗した指紋を回復させる触覚テクスチャセンサ

○ムハマド イルワン ヤンワリ（東京都立大学），岡本 正吾（東京都立大学）*

Tactile texture sensor that heals abraded finger prints

○ Muhammad Irwan Yanwari (TMU), and Shogo OKAMOTO (TMU)

Abstract: Epidermal ridges are crucial for tactile sensing in synthetic sensors. However, these ridges in synthetic sensors are susceptible to abrasion damage after repeated use. Unlike human skin, synthetic sensors cannot heal themselves. To date, healing mechanisms for abraded ridges have not been proposed, and their effectiveness needs to be demonstrated. In this study, a reshaped material was used as a healing mechanism. By heating the material and placing it in a healing mold, we were able to recreate the epidermal ridges. To examine the impact of abrasion damage on synthetic sensors and the effectiveness of the healing mechanism, we observed changes in signal levels between sensors with intact, abraded, and healed ridges, and applied these changes to a classification model. Based on our experiment, the abraded sensor lost its sensitivity to fine textures, such as the 1 mm wavelength specimen. This change significantly affected the classification model's performance, reducing its accuracy to 50%. After the healing procedure, we were able to recover some of the sensor's sensitivity, which increased classification accuracy to 90%. These results show the potential for synthetic tactile sensors to be used for extended periods and prevent a decline in sensitivity until it is time for sensor replacement.

1. Introduction

Fingerprints, or epidermal ridges, play a crucial role in human tactile sensing. During surface texture sensing, the ridges generate vibrations when sliding over a rough surface, and these vibrations are transmitted to mechanoreceptors within the skin[1]. The information is then sent to the brain, enabling it to judge the roughness of the object's surface. Many studies on tactile sensors have sought to replicate the structure of the human finger to emulate its sensing function, including features such as a layered structure, epidermal ridges, and it's healing capability.

The human hand has a multi-layered structure, with bone at the center of the finger surrounded by epidermis, dermis and subcutaneous tissue[2]. This structure has inspired tactile sensor design in Lu's research. The surface of the human finger is covered by fingerprints, or epidermal ridges, whose importance is well known in tactile sensor research. It has been shown that epidermal ridges can enhance tactile signals by a factor of 100 in response to vibrations caused by textures for a specific wavelengths[3]. Human epidermal ridges possess a healing mechanism that helps maintain their shape after minor injuries[4), 5)]. In contrast, synthetic tactile sensors lack inherent mechanisms to preserve their structural integrity. Many researchers have tried to emulate the healing capabilities of the human finger. Roels et al. developed a mechanical finger with healing capabilities for cut damage, where large pieces of material could be reattached to the sensor[6]. Tee et al.[7] developed a synthetic skin with healing function for cuts. The skin material in that research was conductive and exhibited pressure-sensitive performance. Abrasion damage differs in this respect, as it leaves behind tiny particles of material rather than large chunks. Abraded sensor also still functions, making this damage hard to identify.

This study explored the impact of ridge abrasion on the sensor and the effectiveness of healing the sensor's ridges to address this issue.

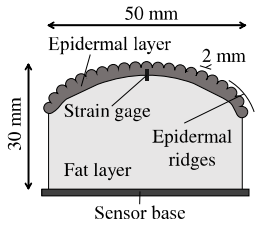

(a) Figure 1 : sensor illustration.

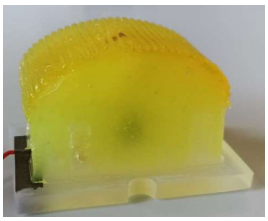

(b) Figure 2 : tactile sensor.

Fig. 1 Sensor design.

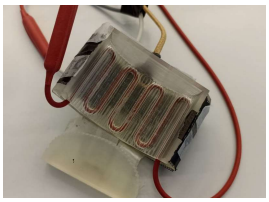

(a) Figure 1 : Ridge mold.

(b) Figure 2 : Healing process.

Fig. 2 Healing procedure.

2. Sensor Design

The structure of the current sensor followed the design of a previous researcher[8), 9)]. The sensor composition is two layers structure designed to imitate the structure of human skin's epidermal and fat tissues. The fat layer has a Young's modulus of 0.17 MPa, while the epidermal layer has a Young's modulus of 0.82 MPa, closely aligning with estimates from anatomical studies of human tissues[10]. Polyvinyl chloride plastisol (Plastic Worm, Two-L Co., Ltd., Japan) was selected as the material due to its manageable hardness. The desired hardness is achieved by adjusting the ratio of softener to hardener in the mixture. The dimensions of the tactile texture sensor are as follows: 50 mm in length, 30 mm in width, and 30 mm in height, with the sensor's base measuring as follows:

* This study was in part supported by Suzuki Foundation.

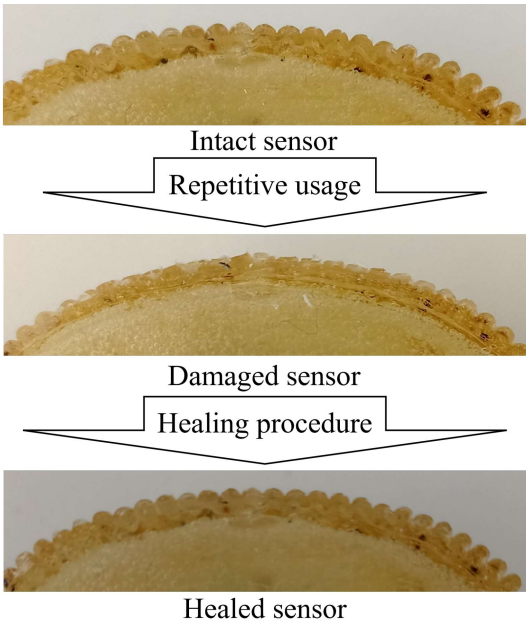

Fig. 3 Ridges condition.

60 mm in length, 40 mm in width, and 5 mm in height, as illustrated in **Fig. 1(a)**. The outer half of the sensor is circular, resembling a human fingertip, and features a raised pattern on the epidermal layer to simulate the functionality of epidermal ridges.

The ridges are 2 mm in size, which is approximately four to five times larger than the ridges of an adult human finger ridges[11], These ridges will be downsized in future iterations. In this study, the term "intact sensor" refers to the condition where the ridge structure remains unchanged, "damaged sensor" refers to a condition where the ridges are flattened, and "healed sensor" refers to a condition where the ridge structure is restored to a state similar to that of the intact sensor after the damaged ridges have healed, as shown in **Fig. 3**.

The tactile sensor incorporates a strain gauge (KFGS-1-120-C1-11 L3M2R, Kyowa Electronic Instruments Co. Ltd., Japan) as a transducer to emulate the sensory capabilities of human tactile receptors. The strain gauge, measuring 1 mm in length, has a gauge factor of 2.10 and a resistance of 119.6 Ω. It is positioned between the inner and outer layers beneath the central ridge. The strain gauge signals are amplified using a dynamic strain amplifier (DPM-913B, Kyowa Electronic Instruments Co. Ltd., Japan). We set the strain gauge configuration to 1500 $\mu\varepsilon$/V.

3. Methods

3.1 Apparatus and Textural Specimens

The specimens used in this experiment were manufactured by 3D-printing techniques (White Resin Form 3+, Formlabs, USA) with surface textures (wavelengths) of 1 mm and 2 mm. The specimen's width and length were 4 cm and 13 cm, respectively.

3.2 Measurement and Healing Procedures

The sensor was mounted on a six-degree-of-freedom articulated robotic arm (MyCobot, Elephant Robotics Co. Ltd., China). It traversed the 13 cm specimen at a velocity of 30 mm/s, while maintaining a constant normal contact force of approximately 1 N. Data acquisition was facilitated by a data acquisition device (USB-6002, National Instruments Co., USA). The scanning process was repeated 1,330 times. The number of scans was not predetermined but was instead based on when the ridges became noticeably flat.

The sensor uses a non-autonomous healing mechanism, specifically heating the material to reshape it. The abraded surface is first cleaned with an industrial paper towel, and then the sensor is placed in healing molds, as shown in **Fig. 2(b)**. These molds are made of heat-resistant resin (High Temp Resin Form 3+, Formlabs, USA), as shown in **Fig. 2(a)**. The mold is connected to a temperature controller (TXN-200AL, As One Co., Ltd., Japan), to adjust the mold temperature. During the healing process, the mold were heated to 70°C for five minutes. After heating, the sensor was retained within the mold until the mold temperature had sufficiently decreased before extraction.

3.3 Data Analysis

Due to the signal amplification capability of epidermal ridges[3], abrasion on the surface of the ridges affects the captured signal levels. By comparing the sensor signals before and after damage, signal deterioration can be estimated.

Since the primary function of the tactile texture sensor is to judge object surfaces, it is necessary to demonstrate how this damage affects the sensor's functionality.

To evaluate functionality, three classification models were used to estimate the impact of sensor abrasion damage: Feed Forward Neural Network (FFNN)[12], K Nearest Neighbor (KNN)[13], and Gradient Boosting Machines (GBM)[14]. The data were classified into two types of texture: 1 mm and 2 mm specimens. The dataset for training the models consisted of 100 measurement samples from each of the 1 mm and 2 mm specimens. The measured data from each sample was transformed into a power spectrum of 1–300 Hz. These training dataset were collected by using the intact sensor.

For testing purposes, 150 measurement samples from each specimen were used, taken from the intact, damaged, and healed sensors. Each sensor provided 50 test samples per specimen. Each model used a frequency spectrum of 1–300 hz as input, and then judged whether the surface wavelength of the scanned specimen would be 1 mm or 2 mm. The FFNN was configured with 10 nodes in the hidden layer. The KNN model used five neighbors to predict the data class. The GBM model was configured with 100 learning cycles and 0.01 learning rates.

4. Results

Fig. 4 and **Fig. 5** show the difference between the amplitude spectra of the intact, damaged, and healed sensors. When the difference value is close to 0 dB, it indicates that the recorded signal is similar to that of the intact sensor. Higher number indicates that the recorded signal is very different to that of the intact sensor. The signal level deterioration after the sensor ridges were abraded is approximately 20 dB for the 1 mm specimen, with the highest peak close to 50 dB. For the 2 mm specimen, the signal level deterioration is approximately 10 dB , with the highest peak reaching 40 dB. After the healing procedure, the signal level increases to some extent,

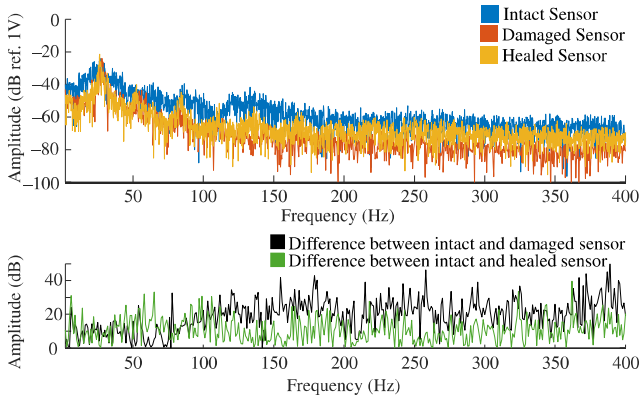

Fig. 4 Intact, damaged, and healed sensor signal for the 1 mm specimen.

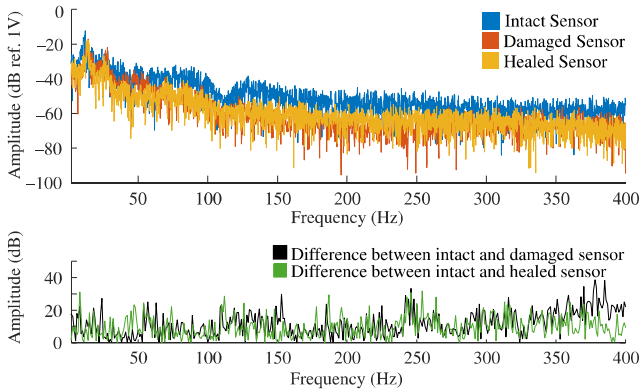

Fig. 5 Intact, damaged, and healed sensor signal for the 2 mm specimen.

as shown in both diagrams. Post-healing, the signal difference between the intact and healed sensors is approximately 10 dB for the 1 mm specimen, with the highest peak close to 40 dB. Some frequencies show improvement, falling below 10 dB. The signal from the 2 mm specimen shows little improvement, with an average signal difference around 10 dB. The highest difference in the 2 mm specimen is close to 30 dB.

The functionality assessment shows a significant decline in accuracy for the damaged sensor, as presented in **Table 1**. The damaged sensor exhibited approximately a 50% reduction in accuracy across the models compared to the intact sensor. The improvement in sensor signals after the healing procedure positively impacts the prediction accuracy. After healing, the highest recorded accuracy was 90%, with an overall accuracy above 60%.

5. Discussion

The epidermal ridges of the tactile texture sensor became abraded after repetitive use, leading to signal degradation. We observed a signal level degradation resulting from this abrasion-induced damage. This decrease in signal level was not uniform across all frequencies, with certain frequencies exhibiting a more significant decline than others. Specifically, frequencies around 400 Hz showed the most prominent drop. In other frequency ranges, the signal deterioration was approximately 20 dB for the 1 mm specimen and 10 dB for the 2 mm specimen. The disparity between the signals recorded from both specimens indicates that smaller wavelengths are more affected by sensor damage than larger wavelengths. This disparity needs to be further examined to determine how small the specimen's wavelength must be for the damage to begin impacting the recorded signal. The weakening of signals across this broad range indicates a decrease in the sensor's sensitivity to subtle differences in textures. This reduction in sensitivity affected the sensor's ability to differentiate between two object surfaces, as shown in Table 1.

Table 1 Accuracy of the three classification models.

Model	Intact sensor	Damaged sensor	Healed sensor
FFNN	100%	50%	75%
KNN	100%	50%	63%
GBM	97%	58%	90%

To address the abrasion problem, a healing procedure for the sensor ridges was implemented in this study. After the healing process, the signal levels recorded from the tactile sensor showed an increase in sensitivity, as shown in Fig. 4 and Fig. 5. The performance of the healed sensor improved the prediction accuracy across all models used in this study. These results indicate that it is possible to prevent signal degradation by healing the sensor's ridges. By regularly healing the sensor, its sensitivity can be preserved until it is time to replace the sensor.

Based on these findings, we suggest further experiments aimed at increasing the effectiveness of the healing procedure. Additionally, we recommend to explore more about abrasion damage and finding the line of how much fine the specimen must be for the damage to begin affect the recorded signal.

6. Conclusion

This study explored the impact of ridge abrasion on the sensor and the effectiveness of healing the sensor's ridges to address this issue. Previous research demonstrated the potential for healing the sensor's ridges from abrasion-induced damage[9]. The restoration of the damaged sensor's ridges showed the ability to recover the sensor's performance to near-peak levels, which positively influenced the results of the surface texture judgement. As a future extension, it would be valuable to explore alternative healing procedures and finding the line of how much fine the specimen must be for the damage to begin affect the recorded signal.

References

[1] N. Bai et al. A robotic sensory system with high spatiotemporal resolution for texture recognition. Nature Communications 14.1, (2023). DOI: 10.1038/s41467-023-42722-4.

[2] X. Lu et al. Design of biomimetic human-skin-like tactile flexible sensor. Sensor Review 39.3, pp. 397–406, (2019). DOI: 10.1108/SR-01-2018-0007.

[3] J. Scheibert et al. The role of fingerprints in the coding of tactile information probed with a biomimetic sensor. Science 323.March, pp. 1503–1506, (2009).

[4] L. S. Penrose and P. T. Ohara. The development of the epidermal ridges. Journal of Medical Genetics 10.3, pp. 201–208, (1973). DOI: 10.1136/jmg.10.3.201.

[5] K. L. Monson et al. The permanence of friction ridge skin and persistence of friction ridge skin and impressions: A comprehensive review and new results. Forensic Science International 297, pp. 111–131, (2019). DOI: 10.1016/j.forsciint.2019.01.046. URL: https://doi.org/10.1016/j.forsciint.2019.01.046.

[6] E. Roels et al. An interdisciplinary tutorial: A self-healing soft finger with embedded sensor. Sensors 23.2, (2023). DOI: 10.3390/s23020811.

[7] B. C. Tee et al. An electrically and mechanically self-healing composite with pressure- and flexion-sensitive properties for electronic skin applications. Nature Nanotechnology 7.12, pp. 825–832, (2012). DOI: 10.1038/nnano.2012.192.

[8] S. Okamoto et al. Roughness feeling telepresence system on the basis of real-time estimation of surface wavelengths. *IEEE/RSJ International Conference on Intelligent Robots and Systems*. (2007), pp. 2698–2703.

[9] M. I. Yanwari and S. Okamoto. Healing Function for Abraded Fingerprint Ridges in Tactile Texture Sensors. Sensors 24.13, p. 4078, (2024). DOI: https://doi.org/10.3390/s24134078.

[10] T. Maeno, K. Kobayashi, and N. Yamazaki. Relationship between structure of finger tissue and location of tactile receptors. Transactions of the Japan Society of Mechanical Engineers. C 63, pp. 881–888, (1997).

[11] H. Cummins, W. J. Waits, and J. T. McQuitty. The breadths of epidermal ridges on the finger tips and palms: A study of variation. American Journal of Anatomy 68.1, pp. 127–150, (1941). DOI: 10.1002/aja.1000680106.

[12] A. Jahagirdar and R. Phalnikar. Comparison of feed forward and cascade forward neural networks for human action recognition. Indonesian Journal of Electrical Engineering and Computer Science 25.2, p. 892, (2022). DOI: http://dx.doi.org/10.11591/ijeecs.v25.i2.pp892-899.

[13] C. G. Evitania. Implementation of the K-Nearest Neighbor Algorithm to Predict Air Pollution. Information Technology and Systems 1.1, pp. 45–54, (2023). DOI: http://dx.doi.org/10.58777/its.v1i1.123.

[14] V. A. Dev and M. R. Eden. Gradient Boosted Decision Trees for Lithology Classification, pp. 113–118, (2019). DOI: http://dx.doi.org/10.1016/B978-0-12-818597-1.50019-9.